Volume 1 | Number 1 | Jan 2013 | Pages 1–100

MedChemComm

www.rsc.org/medchemcomm

pDOS

pFLT3
FLT3

ROYAL SOCIETY OF CHEMISTRY

EFMC
European Federation for Medicinal Chemistry

This is an *Accepted Manuscript*, which has been through the Royal Society of Chemistry peer review process and has been accepted for publication.

Accepted Manuscripts are published online shortly after acceptance, before technical editing, formatting and proof reading. Using this free service, authors can make their results available to the community, in citable form, before we publish the edited article. We will replace this *Accepted Manuscript* with the edited and formatted *Advance Article* as soon as it is available.

You can find more information about *Accepted Manuscripts* in the **Information for Authors**.

Please note that technical editing may introduce minor changes to the text and/or graphics, which may alter content. The journal's standard **Terms & Conditions** and the **Ethical guidelines** still apply. In no event shall the Royal Society of Chemistry be held responsible for any errors or omissions in this *Accepted Manuscript* or any consequences arising from the use of any information it contains.

ARTICLE

Neuronal selective targeting, protection and signaling network analysis via dopamine mediated mesoporous silica nanoparticle

Hailong Zhang [a], Yuhua Jiang [b], Sheng-gang Zhao [c], Li-qin Jiang [c], Yan Meng [d], Peng Liu [e], Myeong Ok Kim [f], Shupeng Li [a, b]

Neuronal transmitters specifically recognize and bind to receptors and exert critical physical and pathological roles in neuronal functions. The possibility to use neurotransmitters as targeting ligand for central nervous system (CNS) drug delivery in nanoparticles has yet to be investigated. To examine the potential of neurotransmitter ligands to target specific neuronal groups, we grafted dopamine to mesoporous silica nanoparticles (DA-MSNs), which enabled highly specific targeting of dopaminergic neuroblastoma SH-SY5Y cells, but not dopamine receptors (DARs) negative cells (HEK293). Antioxidant peptide glutathione (GSH) encapsulated DA-MSNs exhibited higher efficacy as shown by selective protective effects against dopamine toxicity via delivering GSH into dopaminergic cells. Moreover, quantitative mass spectrometry analysis was employed to uncover the dynamic map of proteome changes with/without GSH encapsulated MSN@DA treatment. Several biological pathways were re-wired from proteome interaction networks and revealed important molecules underlying cellular apoptosis caused by dopamine toxicity. These results provide not only a novel way to selectively target specific neuronal groups such as dopaminergic neurons, but also a new tool to ultimately reveal the dynamic changes of proteins involved in various neurological conditions.

Introduction

Nanomaterials have been widely studies during the past decade as a novel drug carrier to construct drug delivery systems (DDSs) for targeted drug delivery and controlled drug release[1]. Among them, mesoporous silica nanoparticles (MSNs) have attracted great interest as one of the most promising inorganic drug carriers. MSNs have unique physicochemical and biochemical stability, tunable particles and pore size, large surface area and pore volume, surface functionalization, good biocompatibility and low cytotoxicity[2]. These features enables MSN-based DDSs significantly higher drug delivery efficacy and time compared to corresponding free drugs. Moreover, many studies involved in ligand-targeted nanomedicines, which mainly choose EGFR[3], HER2[4], folic acid[5] and PSMA[6] as targeting tool, have been investigated in the strategy of tumor treatment. Ligand-targeted MSNs present several advantages over non-ligand targeted MSNs. First, ligand-targeted approaches are more effective compared to encapsulated drugs or ligand-lacking nanomedicines as they improve drug delivery to specific intracellular location via receptor-mediated transcytosis. Second, ligand-targeted MSNs may prove beneficial in increasing drug exposure due to increased target

cell uptake and target tissue retention compared to ligand-lacking MSNs. Finally, Noticeable enhancement of the local drug concentration in the ideal tissue allow lower administration amount to minimize drug-originated systemic toxic effects without compromising therapeutic efficacy.

Dopamine (DA) is a crucial catecholamine neurotransmitter that is widely distributed in mammalian brain. As a chemical messenger, it plays a pivotal role in various functions of the cardiovascular, hormonal, renal systems, especially the central nervous system. Pathologically, the neurotoxicity of DA has been described both in vivo and in vitro studies and is supposed to play an etiologic role in neurodegenerative disorders such as Parkinson's disease (PD)[7]. The exact mechanism of DA's cytotoxic effects is still unknown. Various results have revealed that DA exerts its toxic effect by generation of reactive oxygen species (ROS)[8]. DA is metabolized by different enzymes including mitochondrial monoamine oxidase. On DA terminal injury, it redistributes from synaptic vesicles to cytoplasmic compartments, consequently elevating cytosolic oxidizable DA concentrations. DA also readily undergoes auto-oxidation with formation of neurotoxic metabolites such as quinine species and hydrogen peroxide at neutral pH, which can be reduced into cytotoxic hydroxyl radicals. Both enzymatic metabolism and

auto-oxidation were shown to generate reactive oxygen species (ROS) e.g., superoxide and hydrogen peroxide, reactive nitrogen species (RNS) and induce oxidative stress. Excessive formation of ROS lead to glutathione (GSH) depletion, lipid peroxidation, oxidative damage of DNA, enhanced superoxide activity, and subsequent cellular apoptosis. These pathological processes resulting from oxidative metabolism of DA are considered leading etiological factors in PD pathology[9].

As oxidative stress induced DAergic cell loss is the key pathological processes in PD, antioxidants would be the priority therapeutic to ameliorate oxidative stress, prevent free radical-mediated cellular loss, and inhibit the early degenerative molecular events in PD and its experimental models[10]. GSH, a major cellular antioxidant, participates in various enzymatic and nonenzymatic processes that protect cells against oxidative stress. GSH depletion synergistically increases the selective toxicity of MPP1 in DA cell cultures, and of 6-OHDA and MPTP in vivo[11]. Also, decreased GSH may predispose cells to the toxicity of other insults that are selective targets for dopaminergic neurons. However, although the protective effects of various antioxidants including GSH to modulate oxidative stress in experimental animal models of PD have been reported, antioxidants and supplements appear to have a limited role in the prevention or treatment of PD in clinical trials[12]. Critical factors affecting the efficacy antioxidant therapy include the optimum concentrations required, biologically active forms are needed, efficiency of these agents to cross blood brain barrier to exert potential therapeutic benefits are indeed essential.

Current targeted drug delivery are extensively investigated on various approaches by using different ligands such as antibodies or their fragments, peptides, glycoproteins, carbohydrates, or synthetic polymers[13], and all biocompatible materials for delivery system are constructed according to chemical technology and biochemical principles alone. However, cells constantly rewire and coordinate its intracellular pathways in respond to external stimulus. Elucidating dynamic intracellular protein changes of cellular events will be also crucial to understand how cells respond to the stimulus and how specific pathways are organized, eventually benefit to developing a more efficient targeted drug delivery systems with lower side effect. Herein, to explore a novel protective procedure for DAergic neuronal toxicity, we have employed a novel DA-targeted MSN approach, where GSH as protective reagent. As GSH could not enter the cells by itself, the DA functionalized MSNs offered a selective binding of MSNs to DAergic neurons and thus provides a crucial mean for GSH to localize intracellularly for therapeutic activity against cell death by dopamine insult (Figure 1). Furthermore, quantitative mass spectrometry was used to reveal the dynamic map of proteome changes. The potential biological processes involved in dopamine exposure and GSH delivery by MSNs were analyzed to explore how cells use delivered GSH defense against dopamine insult. By combining label free quantitative mass spectrometry and proteins network analysis software technology, we could uncover biological processes under various cellular states and thus provide a unique insight into the details of the cellular response to dopamine stimulus and molecular mechanism of antioxidant defenses as well as a useful information to improve nanoparticles based drug delivery system.
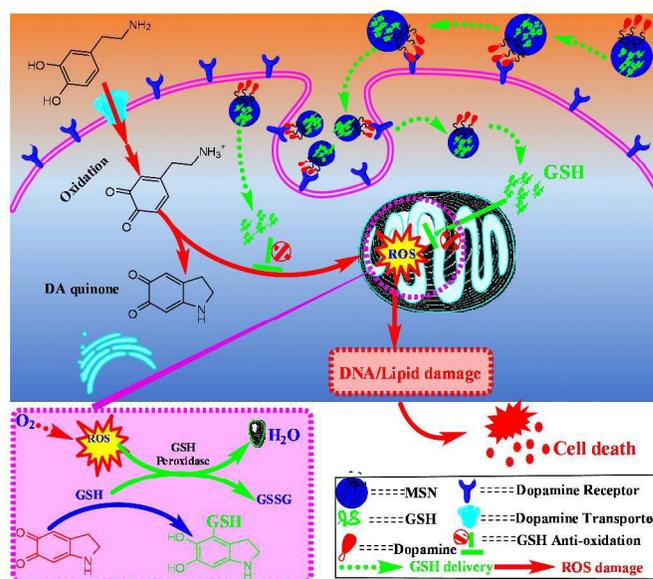

Figure 1.

Figure 1. Schematic illustration of oxidative cytotoxicity caused by dopamine insult, dopamine receptor mediated Glutathione (GSH) delivery by functionalized mesoporous silica nanoparticles (MSNs) and antioxidant defense mechanism of GSH in specific dopaminergic neuronal cells. Solid red line route: Excessive dopamine is uptaken by dopamine transporter in the neuron and followed by oxidation to produce dopamine quinone and reactive oxygen species (ROS), inducing oxidative stress and DNA and lipid damage, mitochondrial dysfunction, broken cellular integrity, eventually leading to cell death. Green dashed line route: dopamine functionalized MSNs selectively targets on dopaminergic neuronal cells, GSH is delivered into cells via dopamine receptors mediated endocytosis, then GSH is released from GSH and subsequently reduces ROS stress levels to rescue neuron cells from oxidative damage.

Experimental Procedures
Methods

Cetyltrimethyl ammonium bromide (CTAB), tetraethyl orthosilicate (TEOS), toluene (anhydrous), Fluorescein, DAtathione (GSH), Dopamine, 2′,7′-dichlorofluorescein diacetate (DCFDA), Calcein blue and propidium iodide (PI) was obtained from Sigma (St. Louis, MO). Annexin V FITC was from BD Pharmingen™ (San Diego, CA). Dulbecco's modified Eagle's medium (DMEM), fetal bovine serum (FBS), penicillin, and streptomycin were obtained from Gibco BRL (Grand Island, NY). DA was dissolved in sterilized H2O. Antibodies for P53, caspase-3, a-tubulin, and PARP were obtained from Cell Signaling Technology (Danvers, MA) and Sigma. Bicinchoninic acid protein assay kit and ECL chemiluminescence system were obtained from Pierce (Rockford, IL) and GE Healthcare (Piscataway, NJ), respectively. All chemicals and solvents were purchased from commercial sources and were used as received, unless otherwise noted.

Preparation of mesoporous silica nanoparticles (MSNs)

Mesoporous silica nanoparticles were synthesized according to previous report with minor modification[14]. CTAB (1.00 g) was dissolved in 480 mL NaOH solution (15 mM), and then the temperature of the mixed solution was then heated up to 80 oC. 5 mL of TEOS was added dropsies in 10 mins with vigorous stirring to avoid formation of giant particles. The white suspension above was further stirred for another 2 hrs at 80 oC to attain uniform nanoparticles. Formed nanoparticles was collected by centrifuge and washed for four times by deionized water and methanol, respectively. Finally, the removal of the CTAB surfactant from inside of nanoparticles was performed by refluxing for 24 h in methanolic solution (160 mL of methanol and 9.00 mL of HCl (37.4%)) to gain mesoporous silica nanoparticles. The formed MSNs was wash with deionized water and methanol extensively, followed by dried at 60 oC over 48hrs to remove H_2O completely and kept at 4 oC for long storage.

Isocyanate functionalized MSNs

Firstly, 100 mg of prepared MSNs was added into 100 mL of dry toluene with stirring, then 50 μL of isocyanatopropyltriethoxysilane was added dropwise, and the solution was refluxed at N2 atmosphere for 12 h to attain MSNs surface isocyanate functionalization. Then the reacted mixture was filtered to remove toluene and unreacted isocyanatopropyltriethoxysilane, followed by washing with deionized water and ethanol for four times, respectively. Finally, isocyanate functionalized MSNs were achieved by dry at in the vacuum over 72 hrs to remove H2O completely.

Dopamine-functionalized MSNs

100 mg isocyanate functionalized MSNs was dissolved in N,N-Dimethylformamide (anhydrous) in sonication, 50 μL triethylamine and 10mg dopamine were added into above solution and stirred for 24 hrs at RT to attain dopamine functionalized MSNs under N_2 protection. The MSNs solution was centrifuged to remove unreacted dopamine. Then dopamine functionalized MSNs was redissolved in Na_2CO_3 buffer (50mM, pH 8.3) and followed by addition ethylenediamine (200 mM) with stirring for 1hrs to block reactive isocyanate groups in the surface of MSNs. After completely washing by deionized water, dopamine functionalized MSNs was dried in the vacuum and kept in 4 oC with N_2 atmosphere for long storage. The dopamine introduced onto MSN surface was measured in a selective fluorometric assay[15]. To a 1.5 ml Eppendorf tube, 100mg dopamine modified MSN was dissolved in water, then centrifuge 10min at 10, 000×g for 5mins to remove extra water. Later, 200 μL 0.5 μM Calcein blue-Fe (II) complex solution was added and mixed. After centrifugation 2 mins at 10, 000×g, the supernatant was collected. The fluorescence intensity of supernatant was measured at 430 nm by fluorescence spectrophotometer.

Characterization of MSNs

The morphology and mesostructure of nanoparticles were observed via scanning electron microscope (SEM) and transmission electron microscopy (TEM). TEM micrographs were obtained on a JEM-2010 electron microscope with an accelerating voltage of 200 kV and SEM at 10 kV. FT-IR of functional group of MSNs was conducted on FTIR Spectrometer 100 (Perkin Elmer).

GSH release kinetics

Under N_2 protection, 50 mg of MSNs were suspended in 3.0 mL ammonium bicarbonate with 20 mg/mL GSH (pH 7.4) at 37 ºC to investigate the GSH release properties in vitro. At 1, 3, 5, 7, 9, 11, 13, 15, 21, 24, 27, 30, 48 hrs intervals, the supernatant was taken out to measure released GSH concentration by mass spectrometer (Applied Biosystems, Foster City, CA). The spectral counting of the released GSH in the MSNs was measured as a function of incubation time.

Preparation of GSH loaded MSNs

Briefly, GSH was dissolved in 2.0 mL of PBS buffer (pH 7.4) in which O_2 was removed via vacuum to avoid GSH oxidization. 100 mg dopamine-MSNs or MSNs only were suspended in above PBS buffer with GSH (0.1mM) and stirred at room temperature overnight in the N_2 protection. The GSH loading MSNs were collected by centrifugation and washed three times with PBS (O_2 removal) to remove the unloaded GSH.

Cell culture and treatment

Catecholaminergic neuroblastoma SH-SY5Y cells were grown in DMEM supplemented with 10% FBS, 100 U/ml penicillin, and 100 U/ml streptomycin. Cells are cultured in medium at 37 ºC in a 5% CO_2 humidified environment for 48 h and reach the confluence of 80% before employed for experiments. Then, the medium used to culture the cell plates was replaced with media containing 100 μg/mL MSNs, GSH@MSNs, Dopamine-MSN@GSH, free GSH (0.1 mM), followed by treatment with dopamine (100 μM) after 30 minutes. Cells were further incubated with above MSNs, GSH@MSNs, and Dopamine-GSH @ MSN, free GSH and/or dopamine for another 24 hrs. Ninety-six-well culture plates were used for cell death assay. Six-well culture plates were used for the Annexin V-FITC/PI staining, and 35 mm glass bottom dishes were used for confocal laser scanning microscopy (CLSM) imaging.

Immunoblot analysis

The cells treated with or without MSNs, MSN@GSH, Dopamine-MSN@GSH, free GSH and/or dopamine were washed once with ice-cold PBS and then scraped, collected by centrifugation, and lysed using ice-cold RIPA buffer containing protease inhibitor cocktail (Sigma) at 4ºC for 30 min. Cell lysates were centrifuged at 13,000 rpm for 25 min, and the protein concentrations were determined by the bicinchoninic acid method (Pierce) using BSA as standard. For Western blot analysis, 50 μg of the protein lysates were separated by 12% SDS-PAGE and transferred to nitrocellulose membrane (Bio-Rad, Hercules, CA). Membranes were saturated in 5% milk in TBS-T (0.5 M Tris, pH 7.4, 2 M NaCl, and 0.1% Tween 20) and incubated for 1 h at room temperature with antibodies for Caspase-3, P53, PARP, α-tubulin from Cell signaling technology (Beverly, MA, U.S.A), followed by secondary antibodies conjugated with HRP. Images were processed with Image J (NIH, Bethesda, MD) for densitometric quantification;

protein levels were normalized with α-tubulin. All measurements were performed in triplicate.

Dopamine-mediated cytotoxicity

To quantify Dopamine-mediated cell death, culture medium was replaced by extracellular solution containing 50 μg/mL of PI (Invitrogen, Carlsbad, CA). After designated time of incubation at 37ºC, fluorescence images were captured through a monochrome chilled CCD camera and fluorescence intensity in each well was measured with a plate reader (Victor3; Perkin-Elmer, Waltham, MA).

Measurement of reactive oxygen species (ROS)

Intracellular ROS content in cells was visualized using 2,7-dihydrodichlorofluorescein diacetate (DCFH-DA) essentially as described. After incubation with MSNs, MSN@GSH, Dopamine-MSN@GSH, free GSH and/or dopamine, cells was washed with PBS and incubated with media containing 50 μM DCFH-DA for 30 min at 37°C in the dark. After incubation, cells were washed with Locke's solution (pH 7.4) and analyzed under a confocal laser scanning microscope (Fluoview FV 1000, Olympus, Japan). The fluorescence images were taken under a 60X oil-immersion objective. Blue, green, and red luminescent emissions from Hochest 33342, PI, and DCFHDA were excited at the wavelengths of 350, 485 and 530 nm, respectively.

Flow Cytometry Analysis

Cellular apoptosis was evaluated by using flow cytometry with Annexin V-fluorescein isothiocyanate/propidium iodide (Annexin V-FITC/PI) staining. After treatments with 100 uM DA plus 100 μg/mL of MSNs (GSH loaded dopamine-MSNs or free GSH MSNs only) or the equivalent free GSH for 24 h, cells were harvested by incubation with 0.25% trypsin for 5 min and centrifuged at 1500×g for 5 mins, then washed by cold PBS buffer three times. The cells were resuspended in 1× annexin binding buffer (10 mM HEPES, 140 mM NaCl, 2.5 mM CaCl$_2$, pH 7.4) and diluted to around 1×10^6 cells / mL. Then 5 μL of Annexin V-FITC and 2 μL of PI (100 μg / mL) were added into 100 μL cell solution and incubated for 15 min in the dark. The stained cells were assayed by flow cytometry, and data analysis was performed with Win MDI version 2.9.

LC-MS/MS analysis for protein identification and quantification

Cells were harvested by centrifuging 16 000 × g at 4°C for 10 minutes and followed by washing three time with 50 mM NH$_4$HCO$_3$ buffer. Then the cell pellet was disrupted under 50 mM NH$_4$HCO$_3$ with protease inhibitor (1:200 dilution) by probe sonication for 10 × 5 s. The supernatant was collected and total protein content determined with a standard BCA protein assay. 30 μg of above protein sample was used in digestion. Sample was incubated in 5 mM DTT and heated for 10mins at 60ºC, followed by alkylation for 30 min with adding Iodoacetamide (15mM, final) at room temperature in the dark. 1 μg trypsin gold (Trypsin Gold, Mass Spectrometry Grade, Promega, Madison, WI, USA) was added into magnetic beads and incubated overnight at 37 °C under shaking. Then, the reaction was stopped with 1% Trifluoroethanoic acid (TFA, final). Then samples were dried in SpeedVac™ systems

(Thermo Scientific, MA, USA) and stored at -80°C until MS analysis.

A TripleTOF 5600 mass spectrometer (AB SCIEX, Foster City, CA) was used to perform LC-MS/MS analysis using in a data-dependent MS/MS acquisition mode. 100 μL of 3% acetonitrile in 0.1% formic acid was added into tube, and peptides were dissolved for MS analysis with three technical replicates run. 300 μm × 5 mm PepMap100 precolumn (Dionex, Sunnyvale, CA) and a 100 μm × 200 mm analytical column packed with 5 μm Luna C18 (Phenomenex, Torrance, CA) were used to peptide trapping and separation. Gradient was run with 500 nL/min flow rate at 40°C by using H$_2$O and acetonitrile with 0.1% formic acid as mobile phase. Liquid chromatography separation was performed using linear gradient from initial buffer B concentration of 3% to 40% over 90 minutes. Data was collected using for 125 minutes. One-second survey MS spectra were collected (m/z 300−2000) followed by MS/MS measurements on the 3 most intense parent. An exclusion mass width 50 mDa was set as tolerance. Spectra were identified using Analyst QS 2.0 (AB SCIEX) software. Protein Pilot 4.0 (AB SCIEX) was used for relative quantification and protein identification of each triple replicate samples by using the Paragon algorithm. A database of human protein sequences from UniProt was used to protein identification (UniProt KB/Swiss-Prot, released on March 19, 2014: ftp://ftp.uniprot.org/pub/databases/uniprot/current_release/kno wledgebase/proteomes/). Protein quantification was assayed according to contributing peptide ratios calculated by using the chromatogram-based quantitation in Skyline (University of Washington, USA)[16].

Differently expressed proteins biological processes enrichment and analysis

To understand the relationship among differentially expressed proteins and evaluate anti-oxidation of delivered GSH in the cell, biological processes enrichment analysis and interaction network constrcution involved in differently expressed proteins was performed in ClueGO[17]. Significantly expressed proteins (20% above) were picked up from the lists of proteins identified by LC-MS/MS (Supplemental Table S1 and S2). All network diagrams were shown in Cytoscape v. 3.1[18].

Results and discussion

Synthesis and Characterization of Dopamine functionalized MSNs

To specifically target dopaminergic neuronal cells, MSNs with surface modified by dopamine ligand that selectively binds dopamine receptors expressed in neuronal cells has been synthesized. Also, reductive agents of GSH as a payload were employed to protect cells from oxidative stress and cell death. As illustrated in figure 2A, dopamine functionalization of MSNs has been accomplished by two steps: activation of MSNs and dopamine introduction. MSNs were first prepared and then functionalized with dopamine. Then, isocyanate group was introduced to MSN surface with providing amine active group

for dopamine reaction. With calculation by pre-made calibration curve using standard dopamine, the amount dopamine onto the MSN surface was quantified as 130 ± 50 μmol/g. SEM and TEM revealed a cylindrical mesoporous structure with an elongated rod shape (Figure 2B, 2C). Its size distribution was confirmed by TEM with the length and width of 180 and 120 nm, respectively. The catechol structure of dopamine is principal determinant of interaction with dopamine recepors (iDARs). Herein, isocyanate group was firstly introduced onto MSNs surface and then reacted with dopamine via amine group to attain dopamine functionalized MSNs. The bond formation of an isourea between isocynate and amine group from dopamine will leave free catechol structure with providing a stronger interaction between MSN and iDARs in the neuronal cells. The successful introduction of isocyanate group and later dopamine functionalization of MSNs surface were confirmed by FT-IR. The absorption band of Si-O-Si at 1080cm-1 was observed. The introduced isocyanate group showed an absorption band at ~1337 and 2270 cm−1. After dopamine functionalization through isocyanate group grafted on MSNs, the urea group was formed and exhibited an absorption band at 1638 cm-1(CONH) and 1561 cm-1 (N-H) (Figure 2D). The disappeared of absorption at 1337 cm-1 also indicated successful functionalization via isocyanate group.
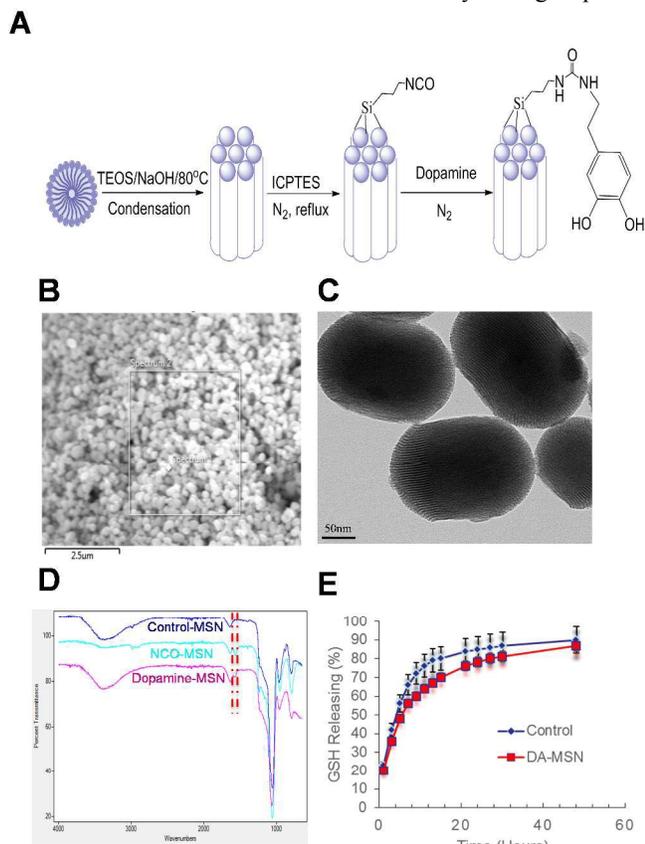

Figure 2

Figure 2. Schematic representation of preparation of mesoporous silica nanoparticles (MSNs) and size characterization. A) Synthetic route of dopamine functionalized

MSNs. B) SEM image of MSNs. C) TEM image of MSNs. D) FT-IR spectra of MSNs: non-functionalized (Control), Isocyanate functionalized (NCO-MSNs) and Dopamine grafted MSNs (Dopamine-MSNs. E) Releasing profiles of GSH from both non-functionalized and Dopamine functionalized MSNs at pH 7.4. The release of GSH was monitored using mass spectrometry with positive mode.

GSH releasing in MSNs

The release assay of the GSH from both non-functionalized and dopamine functionalized MSNs was performed by measurement of released GSH concentration by mass spectrophotometer at m/z 308.0904 after dilution in MS running solution (50% acetonitrile with 0.1% formic acid). As shown in Figure 2E, GSH molecules were effectively entrapped in the pore of dopamine functionalized MSNs with being released for more than 2 days. In non-functionalized MSNs, most of encapsulated GSH (around 80%) release occurred after 15 hrs. However, the functionalization of dopamine exhibits good pore-capping property on showing a slower release in moderation after 30hrs to reach 76% releasing with 15 hrs delays compared to that of non-functionalized MSNs.
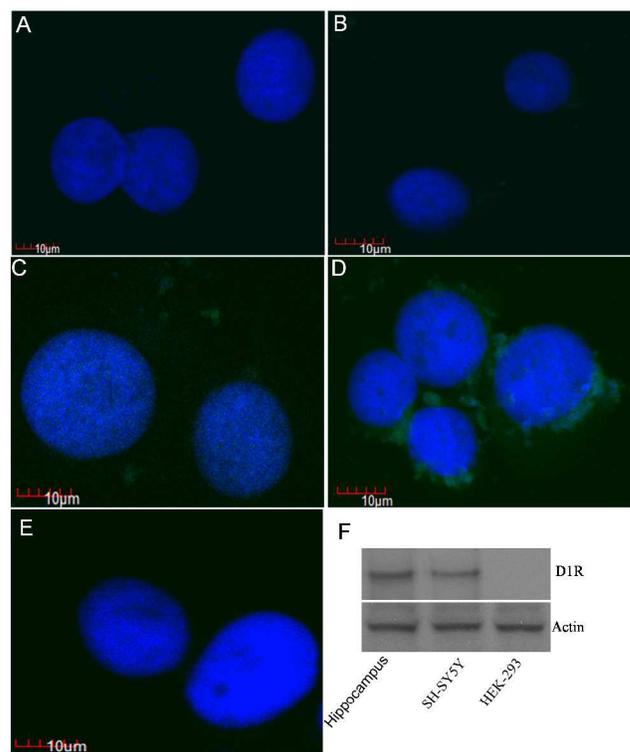

Figure 3

Figure 3: Dopamine conjugated MSN showed specific binding. Confocal microscopy images of HEK-293 (DAR-, A and B) and SH-SY5Y (DAR+, C, D and E) cells after treated with 10 mg/mL of MSN@FITC (A and C) and DA-MSN@FITC (B and D) for 12 hrs. For E, cells are treated with 10 mg/mL DA-MSN@FITC in the presence of 50 uM DA for 12 hrs. Images are taken and merged under green channel from FITC (488/520±10 nm) and blue channel from Hoechst 33258

(340/461 nm±10 nm). For HEK-293 cells where DARs were not expressed, minimal unspedific binding of MSN@FITC or DA-MSN@FITC could be found. For SH-SY5Y cells expressing DARs, massive Glu-MSN@FITC binding both not MSN@FITC could be observed. Expression of DAR1 receptor in SH-SY5Y cells but not in HEK-293 cells was confirmed with western blot analysis (F).

Dopamine mediated targeting to dopaminergic neuronal cells

To examine whether dopamine functionalization of MSNs enables their selective and efficient targeting of dopaminergic neuronal cells, confocal fluorescence microscopy studies were performed using SH-SY5Y human neuroblastoma cell line, which has been widely used as a neuron model to study dopaminergic receptor related neurotoxicity and neuroprotection[19]. Fluorescein was loaded into MSNs to evaluate the cellular uptake of MSNs after incubation with SH-SY5Y and HEK-293 cells (Figure 3). Also, human embryonic kidney (HEK) 293 cell line which does not express DAergic receptor was used as a control system (Figure 3F). Confocal fluorescence microscopy images showed stronger green fluorescence intensity in SH-SY5Y cells treated with dopamine functionalized MSNs (Figure 3D). In contrast, non-dopamine functionalized MSNs treatment groups only showed background fluorescence (Figure 3C). For HEK 293 cells where no dopamine receptor expressed, incubation with both dopamine functionalized or non-dopamine functionalized MSMs either did not show obvious fluorescein staining (Figure 3A, 3B), indicating there is only low nonspecific binding of dopamine functionalized MSNs in dopamine receptor negative cells. Moreover, preincubation with high concentrations of DA blocked the DAR mediated endocytosis of MSNs (Figure 3E). Taken together, these results showed highly specific binding of dopamine functionalized MSNs in dopamine receptor positive cells and clearly demonstrate that the MSNs are taken up by dopamine-mediated endocytosis with negligible nonspecific binding.
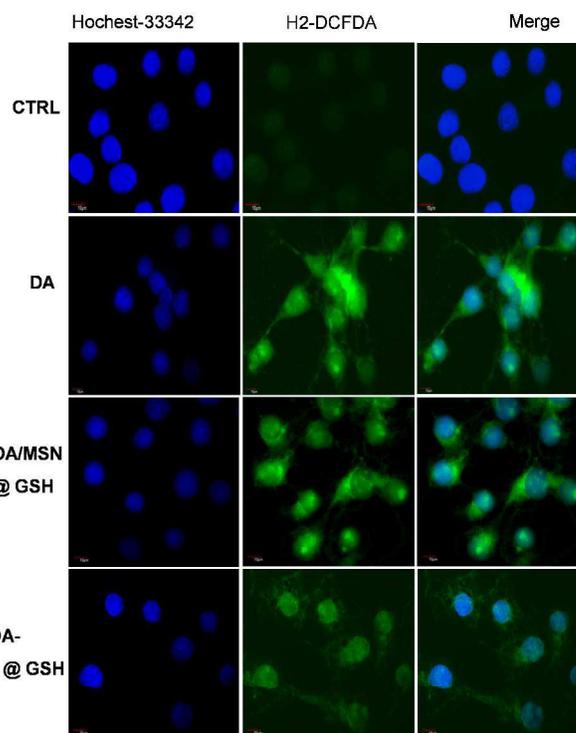

Figure 4

Figure 4. ROS production induced by DA could be ameliorated by DA/DA-MSN@GSH. Intracellular ROS was measured by H2DCFDA fluorescence. Intracellular ROS accumulation by DA and significantly reduced by DA/DA-MSN@GSH but not MSN@GSH. CTRL, control group; DA, dopamine treatment group; DA/MSN@GSH, MSN@GSH and dopamine treatment group; DA/DA-MSN@GSH, DA-MSN@GSH and dopamine treatment group.

ROS inhibition by intracellular delivery of GSH with dopamine@MSNs

Excessive dopaminergic activity has been demonstrated in certain neurodegenerative diseases including Parkinson's disease and Alzheimer's disease. DA exerted its cytotoxic effects, produces reactive oxygen and free radicals, eventually leading to apoptosis. MSNs based GSH delivery system might protect cells from oxidative stresses by virtue of the antioxidant action of their thiols and encapsulated extracts made of polyphenols. To investigate whether MSNs based GSH delivery system could acts as a potent detoxifier against ROS and protect cell from oxidative damage, free GSH, MSNs only, GSH loaded MSNs without dopamine modification and MSNs with surface functionalized by dopamine were incubated with SH-SY5Y cells and then treated with DA to evaluate if GSH delivery could neutralize produced ROS. ROS levels were monitored by DCFH-DA, which produces a fluorescent compound 2,7-dichlorofluorescein (DCF) when met with ROS. As shown in Figure 4 and supplemental figure 1, dopamine induced significant ROS accumulation in SH-SY5Y cells ($206.6 \pm 17.5\%$, compared to controls). Pre-treated by GSH loaded MSNs without dopamine as targeting ligands did not show obvious decrease of intracellular ROS level ($197.7 \pm$

16.1%, compared to controls). However, pre-treatment with GSH loaded MSNs with glutamates as targeting ligands markedly reduced the amount of ROS as shown by the greater decline of fluorescence intensity (114.8 ± 13.8, compared to controls), indicating that intracellular GSH delivery through dopamine functionalized MSNs delivery system showed a higher neuroprotective effects against dopamine elicited ROS production. Interestingly, MSN itself did not cause ROS effects (106.8 ± 9.3 %). Taken together, these results showed that dopamines as targeting ligands for MSNs modification markedly enhanced the GSH cellular delivery efficiency and thus offered much higher antioxidant capacity into DAergic cells of dopamine@MSNs compared to non-targeting MSNs.

Cytoprotective effects of GSH loaded dopamine@MSNs

Dopamine induced ROS could further lead to neuronal apoptosis. To examine whether Dopamine-MSN as delivery tool could offer effectively protective effects against ROS-mediated apoptosis, flow cytometric analysis was performed for qualitative and quantitative determination of cellular apoptosis after GSH encapsulated MSNs pre-treatment by using Annexin V-fluorescein isothiocyanate/propidium iodide (FITC/PI) staining. Dopamine treatment to SH-SY5Y cells for 12 h significantly increased Annexin V positive cells in B2,4 quadrant of the flow cytometric dot-plot, indicating occurrence of apoptosis in SH-SY5Y cell lines exposure to dopamines (Fig. 5A). Dopamine treatment induced a 43.1 ± 3.4% cell death. Pre-incubation of SH-SY5Y cells by GSH loaded MSNs with dopamine as targeting ligand for 12hrs markedly decreased the accumulation of Annexin V positive cells to 17.1 ± 2.2%, whereas GSH loaded non-dopamine MSNs only showed a slight drop to 38.1 ± 3.7% compared to Dopamine treatment without GSH protection (Fig. 5A and Supplemental Fig. 2).

To further examine whether cell apoptotic inhibiting effects of DA-MSNs@GSH could enhance cells survival from dopamine insult, cells death analysis was also performed. Cells are first incubated with MSNs, GSH@MSNs, DA-MSNs@GSH and free GSH for 30 mins, followed by dopamine exposure to the cell medium at the concentration of 100 μM and extended incubation for another 12 hours. Death cells were stained by PI to assess cell viability. As shown in Figure 5B and supplemental Figure 3, remarkable cell death was observed due to dopamine treatment when compared with untreated control SH-SY5Y cell lines without dopamine (178.1±15.6% in dopamine exposure cells compared to control cells). In contrast, the number of dead cells was significantly decreased when SH-SY5Y cells were pre-treated with GSH loaded MSNs with dopamine for targeting before dopamine exposure (119.8% ± 9.7 in cells with pre-treated by GSH loaded dopamine@MSNs). Interestingly, whether SH-SY5Y pre-treatment with free MSN or GSH loaded MSNs without dopamine for targeting did not decline cell death compared to those under dopamine exposure (104.3±6.5% for cells treated with MSN only and 173.7± 10.2 % for cells treated with GSH loaded MSNs as compared to controls, respectively).

Taken together, pre-treatment by dopamine-MSNs loaded with GSH dramatically reduces ROS production, significantly inhibits cell apoptosis and cell death as compared to un-functionalized MSNs. Empty MSNs without GSH did not show obvious cytotoxicity under the same conditions up to a concentration of 100 μg/mL. Dopamine functionalized MSNs developed here could efficiently deliver antioxidants into intracellular SH-SY5Y cells and enhanced protective effects against SH-SY5H cells damage caused by dopamine induced neurotoxicity.
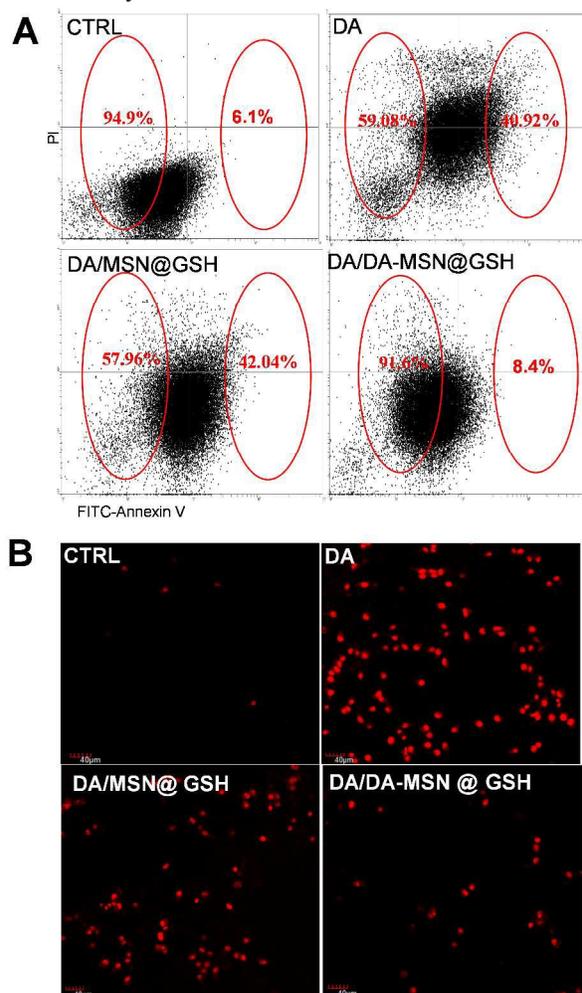

Figure 5

Figure 5. Regulation of the DA-mediated cell death in SH-SY5Y cells. A Flow cytometric analysis of cell apoptotic levels by PI and fluorescence. Results of one representative experiment are shown. The numbers indicate apoptotic cell population in the quadrants indicated by the red ellipse, expressed as a percentage of the total cell population. (A) Shown are the results of FACS analysis of PI and FITC-Annexin V fluorescence. B Propidim iodide (PI) positive cells (red) from SH-SY5Y cells with dopamine treatment in the presence/absence of the DA/MSN@GSH and DA/DA-MSN@GSH, scale bar 40μm. CTRL, control group; DA, dopamine treatment group; DA/MSN@GSH, MSN@GSH and dopamine treatment group; DA/DA-MSN@GSH, DA-MSN@GSH and dopamine treatment group.
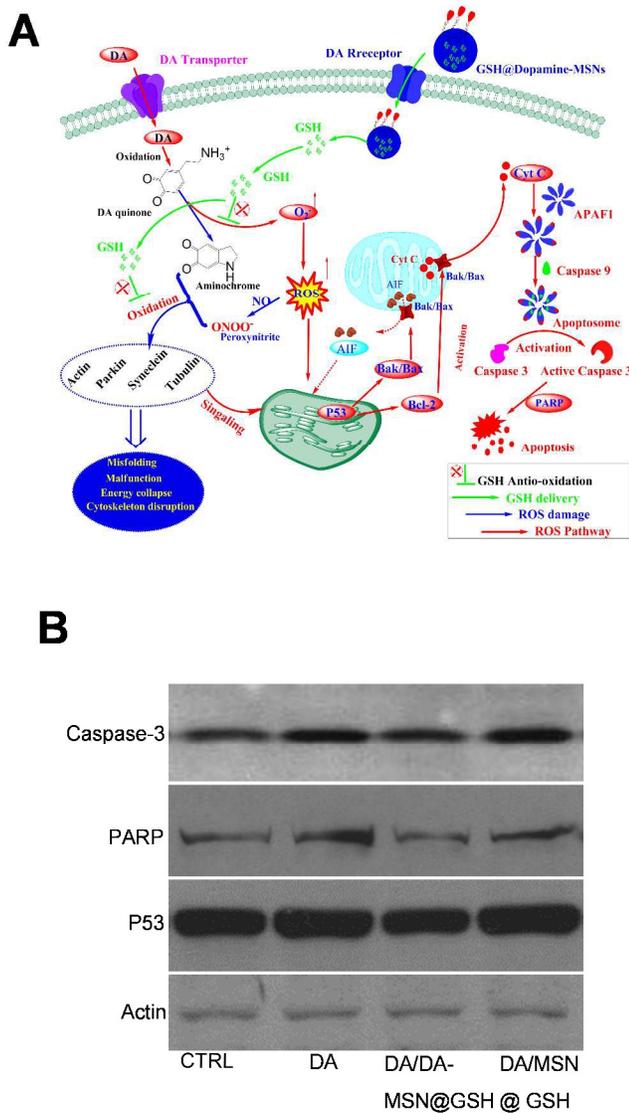
Figure 6

Figure 6. DA/DA-MSN@GSH reduced the expression of apoptotic markers induced by dopamine. **A** Schematic mechanism of possible biological pathways of cell death caused by oxidative dopamine cytotoxicity, GSH loaded MSNs protection against ROS and ROS mediated apoptosis in response to dopamine insult. Excessive dopamine is uptaken by dopamine transporter in the neuron and oxidized to dopamine quinone and aminochrome, producing superoxide radicals, hydrogen peroxide, hydroxyl radicals (reactive oxygen species (ROS)). Oxidative dopamine cytotoxicity disrupts the architecture of the cytoskeleton and mitochondria by formation protein adduct between reactive quinone and ROS and proteins (actin, parkin, syneclein and tubulin), finally cause DNA and lipid damage, mitochondrial dysfunction and cell death. ROS mediated apoptosis is P53 dependent, which regulate PARP activation and result in cellular apoptosis. Cellular delivered GSH by MSN can be oxidized by dopamine quinone and thus maintain intracellular redox homeostasis, rescue cell death from

activation of the apoptotic signaling cascade. **B** Representative western blot assay of proteins in SH-SY5Y cells treated by dopamine in the presence/absence of the DA/MSN@GSH and DA/DA-MSN@GSH.

Anti-apoptotic mechanism of GSH loaded dopamine-MSNs

Dopamine-induced apoptotic cell death associated with caspase-dependent apoptotic pathway (Figure 6A), in which ROS directly causes DNA damage and induces P53 enhanced expression and activation, cytochrome c releasing from the mitochondria into the cytoplasm to form apoptosome by binding apoptotic protease activating factor and caspase 9. Caspase-3, activated by apoptosome, regulates cleavage of Poly-ADP-ribose polymerase (PARP), a 116-kDa DNA repair enzyme, and result in cellular apoptosis. Cellular delivered GSH by MSN can be oxidized by dopamine quinone and thus maintain intracellular redox homeostasis, rescue cell death from activation of the apoptotic signaling cascade. To verify anti-apoptotic mechanism of GSH via inhibition of caspase-dependent apoptotic pathway, the differently expression levels of apoptotic proteins including caspase-3, P53 and PARP were examined by western blot analysis. Also, beta-actin was used as a quantitative control. Representative western blot and quantitative results of respective blot were shown in Figure 6B and supplemental figure 4. All three key proteins caspase-3, P53 and PARP were significantly up regulated when SH-SY5Y cells exposure to dopamine ($153.0\pm6.5\%$, $127.6\pm 6.5\%$,
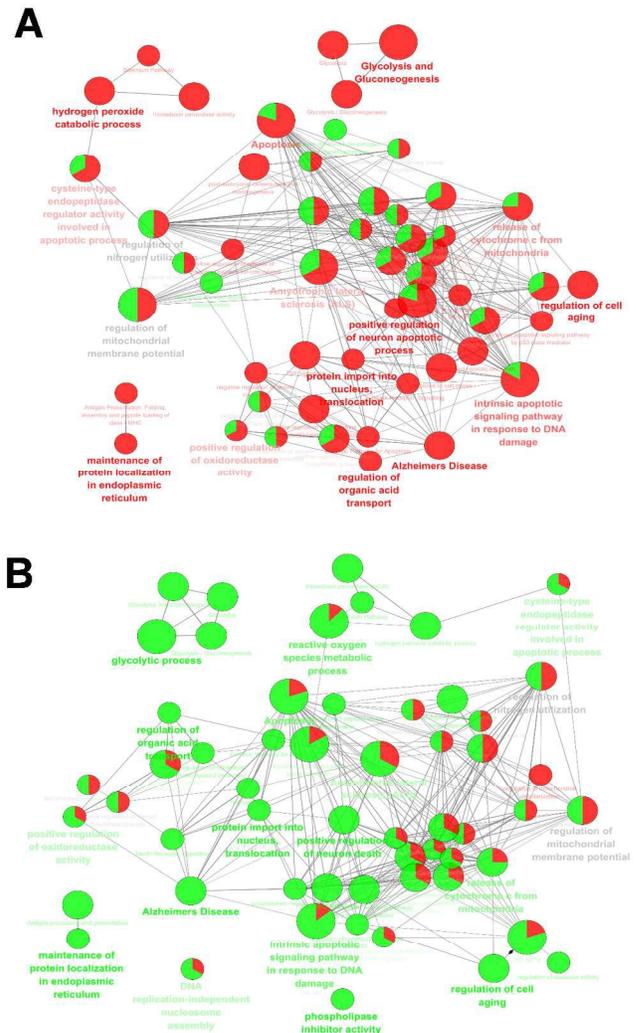

Figure 7

194.1±9.3%, respectively), all of which, in turn, promote further apoptosis and cell death. When treated by GSH loaded MSNs without dopamine for cell targeting, SH-SY5Y did not show obvious decline in those protein expression level (152.4±4.8%, 117.7± 4.6%, 163.2± 5.9%, respectively). Not surprisingly, SH-SY5Y pre-treatment with GSH loaded MSNs with dopamine for targeting efficiently decreased those protein expressions (103.7 ± 8.2%, 101.2±3.9%, 104.9 ± 5.5%, respectively). The result showed that pretreatment with GSH loaded DA-MSNs could inhibit differently expression of caspase-3, P53 and PARP, prevent apoptotic signaling under dopamine exposure and thus protect cell from neurotoxicity. All these results reveal that GSH loaded DA-MSNs system acts as protective reagent against oxidative-mediated apoptosis from dopamine excitotoxicity by neutralizing intracellular ROS level.

Systematic rewiring of dynamic protein networks in response to dopamine neurotoxicity

Figure 7. Schematic illustration of systematic rewiring of dynamic biological network to analyze differently proteins expression in response to dopamine insult and delivered GSH protection in specific dopaminergic neuronal cells. Biological network analysis was performed by with ClueGo and visualized with Cytoscape for those proteins with significantly altered expression levels to identify biological pathways relevant to cytotoxicity by dopamine. Only significantly changed proteins with at least 1.20 fold after dopamine insult or GSH-pretreated before dopamine exposure were chosen to construct biological network. Biological pathways and functions are visualized as colored circular nodes linked with related proteins based on their change of expression level, those terms with up-regulated are shown in green while those with regulated proteins are red, respectively. The color gradient shows the gene proportion of each cluster associated with the term. The node size reflects the enrichment significance of the term and functionally related proteins groups are linked. (A) Biological pathways analysis of significantly changed proteins showing the most significant functional biological pathways altered in dopaminergic neuronal cells under dopamine insult compared with control cells. (B) Biological pathways analysis of significantly changed proteins showing the most significant functional biological pathways altered in dopaminergic neuronal cells with GSH/Glu@MSN pre-treatment before dopamine exposure compared with cells under directly dopamine insult without GSH protection.

Protein expression levels of a biological system are under constant changes in respond to environment. Various effects have been put to understand how cells re-wire the protein network to adjust the stimulus. To date, there are only limited means to elucidate the dynamic proteins networks for central nervous system. MSNs anchored with selective ligand provided a unique way to study neuronal proteomic changes on specific treatment, also offered a systemic analysis tool to elucidate molecular mechanisms of a certain neuronal group. Combining label free quantitative mass spectrometry technology and biological proteins network analysis software, we mapped the global protein expression changes under dopamine exposure with or without GSH protection and examined the molecular mechanism of cellular apoptosis process underlying ROS.

In total, 48 proteins significantly changed under dopamine exposure in all identified and quantified 345 proteins. 28 were up regulated and 20 were down regulated after dopamine insult (Table 1 and supplemental table S1). Molecular function and expression change under dopamine insult with or without GSH protection were analyzed and summarized. 15 molecular functions were harmed due to dopamine insult: actin & calmodulin-binding, anion transport, apoptosis regulation, ATP & nucleotide binding, calcium ion homeostasis, carbohydrate degradation, cell adhesion, cell redox homeostasis, chaperone, chromatin binding, cytokine activity, protein methylation, regulation of cell growth & proliferation, regulation of dopamine release and transport, transcriptional regulation. 40 (83% of total differently expressed proteins) were recovered when pretreated with DA-MSN@GSH, whereas 8 proteins did not change expression trend (half were recovered but not significantly). Then biological pathways of these differently expressed proteins were analysed by the GO enrichment using the DAVID[20] (Shown in Supplemental Table S2). Most significant biological processes and associated proteins identified under dopamine exposure were listed in table 2. Pretreatment with GSH selectively recovered 16/18 biological pathways involved in Alzheimers Disease, Amyotrophic lateral sclerosis (ALS), apoptosis, cysteine-type endopeptidase regulator activity involved in apoptotic process, glycolytic process, intrinsic apoptotic signaling pathway in response to DNA damage, maintenance of protein localization in endoplasmic reticulum, positive regulation of neuron death, positive regulation of oxidoreductase activity, protein import into nucleus, translocation, reactive oxygen species metabolic process, regulation of cell aging, regulation of mitochondrial membrane potential, regulation of nitrogen utilization, regulation of organic acid transport, release of cytochrome c from mitochondria. Only two pathways failed to be recovered by GSH protection: DNA replication-independent nucleosome assembly and phospholipase inhibitor activity.

To directly view the global protein changes, proteomic network analysis was performed using ClueGo and visualized with Cytoscape for those proteins with significantly altered expression levels to identify biological processes relevant to cytotoxicity by dopamine. Only significantly changed proteins with at least 1.20 fold after dopamine insult or GSH-pretreated before dopamine exposure were chosen to construct biological network (Figure 7). Down-regulated biological processes and functions are visualized as red under dopamine treatment (Figure 7A). When pretreated with GSH loaded DA-MSNs, SH-SY5Y cells restored most of biological processes and marked by green (Figure 7B). Only few biological processes triggered by dopamine insult did not recover (table 2 and figure 7). These results showed proteomic changes of neuronal

responses to dopamine insult and the protective mechanisms of GSH to reduce ROS level and rescue cell death.

Taken together, our experimental results (Figure 4-6) and biological pathways analysis of differentially expressed proteins (Figure 7, Table 1 and 2) have shown consistent result: most of differentially expressed proteins and biological pathways under dopamine insult are involved in ROS mediated cellular apoptosis; pretreatment with antioxidant GSH loaded MSNS was able to protect SH-SY5Y through neutralizing ROS level and thus avoided ROS mediated cellular apoptosis via ROS-dependent pathway. If antioxidant peptide GSH could inhibit ROS accumulation in response to dopamine stimuli, not surprisingly, all differentially expressed proteins and biological pathways involved in ROS will be recovered. Also, the general view of various biological processes involved dopamine excitotoxicity supported our biological processes analysis and summarized to elucidate how GSH cellular delivery via DA-MSNs protects cells against ROS and ROS mediated cell death.

Conclusions

This study evaluated a MSNs based neuronal cell targeted delivery system, which rescued dopamine induced ROS production, neurotoxicity and apoptotic cell death. To specifically recognize dopaminergic neuronal cells, the target ligand of dopamine was grafted onto MSNs surface. Confocal immunofluence microscope imagination revealed dopamine functionalized MSNs but not un-functionalized MSNs specifically bound and were up-taken by DARs expressed in SH-SY5Y cells, whereas HEK293 cells without dopamine receptor failed to uptake DA functionalized MSNs, indicating that DA-MSNs selectively targeting to SH-SY5Y is mediated by DA-DARs interaction. To examine the protective efficacy of dopamine-MSNs based delivery system, a reductive reagent GSH was loaded and its protective mechanism against dopamine induced oxidative stress and neuronal apoptosis were studied. In vivo cell analysis found that dopamine-MSN@GSH significantly reduced the accumulation of intracellular ROS. Furthermore, dopamine-MSN@GSH exhibited a highly efficient protection against dopamine induced cell apoptotic as determined qualitatively and quantitatively by confocal microscopy and flow cytometric analysis. Moreover, dopamine-MSN@GSH restored cell apoptotic protein marker expressions back very close to psychological state but not non-dopamine functionalized MSNs. Finally, global protein analysis was performed to investigate the specific protective mechanisms of dopamine-MSNs against dopamine neurotoxicity. Protein network analysis revealed that proteins belonging to different biological processes are dynamically regulated due to dopamine insult and can be restored effectively by GSH pre-treatment. Our study not only provided an alternative strategy for the treatment of neurological disease resulting from specific neurotransmistters such as Parkinson's disease and Alzheimer's disease, but also reveals the underlying mechanisms of anti-

apoptotic effects of GSH cellular delivery via MSNs which specially offers promising information to develop a highly efficient drug delivery system with lower side effect. Furthermore, neuronal specific targeting MSNs could be used a powerful tool to analyze the intracellular molecular mechanism of a certain neuronal groups.

Notes and references

[a] Laboratory of Clinical Chemistry & Drug Innovation, The Second Hospital of Shandong University, Jinan, Shandong 250033, P.R. China

[b] Cancer Centre, The Second Hospital of Shandong University, Jinan, Shandong 250033, P.R. China

[c] Department of Cardiology, The Second Hospital of Jiaxing, Jiaxing, Zhejiang 314000, P.R. China

[d] Department of Urology, The Second Hospital of Shandong University, Jinan, PR China.

[e] Department of Chemistry, University of Toronto, Toronto, Canada

[f] Division of Life Science and Applied Life Science (BK21 plus), College of Natural Sciences, Gyeongsang National University, Jinju, 660-701, Republic of Korea

*Correspondence to: Shupeng Li (E-mail: sdeylsp@gmail.com), Cancer Centre, The Second Hospital of Shandong University, 247 Beiyuan Street, Jinan, Shandong, 250033, P.R. China. Or Myeong Ok Kim (E-mail: mokim@gnu.ac.kr), Division of Life Science and Applied Life Science (BK21 plus), College of Natural Sciences, Gyeongsang National University, Jinju, 660-701, Republic of Korea

Electronic Supplementary Information (ESI) available: [supplemental figures and tables are available online].

1. R. van der Meel, L. J. Vehmeijer, R. J. Kok, G. Storm and E. V. van Gaal, *Advanced drug delivery reviews*, 2013, **65**, 1284-1298.
2. V. Mamaeva, C. Sahlgren and M. Linden, *Advanced drug delivery reviews*, 2013, **65**, 689-702.
3. C. Mamot, R. Ritschard, A. Wicki, G. Stehle, T. Dieterle, L. Bubendorf, C. Hilker, S. Deuster, R. Herrmann and C. Rochlitz, *The Lancet. Oncology*, 2012, **13**, 1234-1241.
4. J. W. Park, D. B. Kirpotin, K. Hong, R. Shalaby, Y. Shao, U. B. Nielsen, J. D. Marks, D. Papahadjopoulos and C. C. Benz, *Journal of controlled release : official journal of the Controlled Release Society*, 2001, **74**, 95-113.
5. A. Krais, L. Wortmann, L. Hermanns, N. Feliu, M. Vahter, S. Stucky, S. Mathur and B. Fadeel, *Nanomedicine : nanotechnology, biology, and medicine*, 2014, **10**, 1421-1431.
6. B. Huang, J. Otis, M. Joice, A. Kotlyar and T. P. Thomas, *Biomacromolecules*, 2014, **15**, 915-923.
7. M. Asanuma, I. Miyazaki and N. Ogawa, *Neurotoxicity research*, 2003, **5**, 165-176.

MedChemComm Accepted Manuscript

8. C. C. Chiueh, T. Andoh, A. R. Lai, E. Lai and G. Krishna, *Neurotoxicity research*, 2000, **2**, 293-310.

9. V. Dias, E. Junn and M. M. Mouradian, *Journal of Parkinson's disease*, 2013, **3**, 461-491.

10. I. Miyazaki and M. Asanuma, *Neurochemical research*, 2009, **34**, 698-706.

11. M. Smeyne and R. J. Smeyne, *Free radical biology & medicine*, 2013, **62**, 13-25.

12. M. Lohle and H. Reichmann, *Journal of the neurological sciences*, 2010, **289**, 104-114.

13. T. M. Fahmy, S. L. Demento, M. J. Caplan, I. Mellman and W. M. Saltzman, *Nanomedicine (Lond)*, 2008, **3**, 343-355.

14. D. R. Radu, C. Y. Lai, K. Jeftinija, E. W. Rowe, S. Jeftinija and V. S. Lin, *Journal of the American Chemical Society*, 2004, **126**, 13216-13217.

15. D. Seto, T. Maki, N. Soh, K. Nakano, R. Ishimatsu and T. Imato, *Talanta*, 2012, **94**, 36-43.

16. B. Schilling, M. J. Rardin, B. X. MacLean, A. M. Zawadzka, B. E. Frewen, M. P. Cusack, D. J. Sorensen, M. S. Bereman, E. Jing, C. C. Wu, E. Verdin, C. R. Kahn, M. J. Maccoss and B. W. Gibson, *Mol Cell Proteomics*, **11**, 202-214.

17. G. Bindea, B. Mlecnik, H. Hackl, P. Charoentong, M. Tosolini, A. Kirilovsky, W. H. Fridman, F. Pages, Z. Trajanoski and J. Galon, *Bioinformatics*, 2009, **25**, 1091-1093.

18. P. Shannon, A. Markiel, O. Ozier, N. S. Baliga, J. T. Wang, D. Ramage, N. Amin, B. Schwikowski and T. Ideker, *Genome research*, 2003, **13**, 2498-2504.

19. C. Gomez-Santos, I. Ferrer, A. F. Santidrian, M. Barrachina, J. Gil and S. Ambrosio, *Journal of neuroscience research*, 2003, **73**, 341-350.

20. W. Huang da, B. T. Sherman and R. A. Lempicki, *Nature protocols*, 2009, **4**, 44-57.

MedChemComm Accepted Manuscript